Pflügers Arch - Eur J Physiol (2002) 444:276–285
DOI 10.1007/s00424-002-0811-3

ORIGINAL ARTICLE

Meng-Ru Shen · Paola Furla · Cheng-Yang Chou
J. Clive Ellory

Myosin light chain kinase modulates hypotonicity-induced Ca^{2+} entry and Cl^- channel activity in human cervical cancer cells

Received: 5 December 2001 / Revised: 24 January 2002 / Accepted: 25 January 2002 / Published online: 6 March 2002
© Springer-Verlag 2002

Abstract Hypotonicity-induced Ca^{2+} entry is a critical signal for the normal regulatory volume decrease in human cervical cancer cells. The aim of this study was to explore the role of myosin light chain kinase (MLCK) in the regulation of hypotonicity-induced Ca^{2+} signalling and Cl^- channel activity. Blockade of MLCK activity by $MLCK_{(11–19)}$ amide, a substrate-specific peptide inhibitor, markedly attenuated hypotonicity-induced Ca^{2+} entry. A similar result was obtained with ML-7, a synthetic naphthalenesulphonyl derivative that inhibits the binding of ATP to MLCK. More than 85% of the activity of the volume-regulated Cl^- channel was suppressed when intracellular Ca^{2+} was buffered to near zero in the absence of extracellular Ca^{2+}, suggesting that hypotonicity-induced Ca^{2+} signalling is important for the activation of the volume-regulated Cl^- channel. Intracellular dialysis with $MLCK_{(11–19)}$ amide or ML-7 concentration-dependently reduced the amplitude and rate of activation of the volume-regulated Cl^- channel. Swelling-activated taurine transport was also inhibited concentration dependently by ML-7 and $MLCK_{(11–19)}$ amide with IC_{50} values of 6.4 and 2.0 μM, respectively. Hypotonicity induced MLC phosphorylation which was mediated totally by MLCK and depended on Ca^{2+} entry. However, phosphorylated MLC per se was not involved critically in the regulation of Ca^{2+} entry and activation of volume-sensitive organic osmolyte/anion channels (VSOAC). We propose that MLCK has a novel function in regulating the activation of VSOAC by mediating Ca^{2+} entry in response to hypotonicity. This function of MLCK on Ca^{2+} signalling does not correlate with MLC phosphorylation.

M.-R. Shen · P. Furla · J.C. Ellory (✉)
University Laboratory of Physiology, Parks Road, Oxford, OX1 3PT, United Kingdom
e-mail: clive.ellory@physiol.ox.ac.uk
Tel.: +44-1865-272436, Fax: +44-1865-272488

M.-R. Shen · C.-Y. Chou
Department of Obstetrics and Gynaecology, College of Medicine, National Cheng Kung University, Tainan 704, Taiwan

Keywords Ca^{2+} · Myosin light chain kinase · Volume regulation · Cervical cancer

Introduction

Volume regulation is a physiological process of fundamental importance to most cell types. Cells defend themselves against hypotonic stress by losing solutes together with osmotically obligated water, a process termed regulatory volume decrease (RVD). The principal solutes lost in RVD are K^+, Cl^- and a variety of largely uncharged or zwitterionic organic solutes, such as taurine [1]. The predominant pathway for RVD in most cell types is the opening of separate K^+ and anion channels [2]. The volume-sensitive organic osmolyte/anion channel (VSOAC) has attracted wide interest because of its role in important cellular functions, including volume regulation, control of membrane potential, pH homeostasis, transport of organic osmolytes and amino acids and cell proliferation [3, 4]. We have demonstrated previously that the activity of VSOAC, which leads to Cl^- and taurine efflux, is strongly up-regulated during human cervical carcinogenesis [5, 6, 7, 8]. The cell cycle progression of cervical cancer cells is also accompanied by differential activities of VSOAC [9, 10].

Hypotonic cell swelling triggers an increase in intracellular $[Ca^{2+}]$ ($[Ca^{2+}]_i$) that is deemed responsible for the subsequent RVD in cervical cancer cells [10, 11, 12]. However, the mechanisms underlying the regulation of hypotonicity-induced Ca^{2+} signalling remain ill-defined. Activation of myosin light chain kinase (MLCK) and the resultant phosphorylation of myosin light chain (MLC) are considered key events in cytoskeletal remodelling, including cell adhesion, spreading and motility [13]. Involvement of MLCK in intracellular signal transduction, however, has classically been restricted to events associated with cell contraction and morphological changes that contribute to cell-cell gap formation and increased permeability in response to various stimuli [14, 15]. Although it is often stated that MLC is the only known sub-

strate for MLCK, agents that affect MLCK activity modulate ionic currents in some cell types [16, 17]. Furthermore, MLCK has a novel function in regulating endothelial Ca^{2+} entry and mediating vasodilation in response to shear stress [18, 19].

VSOAC can be activated by shear stress [20]. It is likely that this pathway needs a linkage to the cytoskeleton which will induce changes in cell shape and possibly folding and unfolding of the membrane. The present study was designed to explore the possibility that MLCK is involved in the RVD response of human cervical cancer cells. The results revealed a novel function of MLCK in affecting Ca^{2+} entry in response to hypotonic shock. The activation of VSOAC could be also modulated by MLCK activity.

Materials and methods

Cell culture

SiHa cells, a human cervical cancer cell line, were obtained from the American Type Culture Collection (Rockville, Md., USA) and maintained at 37 °C in a CO_2-air (5%–95%) atmosphere and cultured in Dulbecco's modified Eagle's medium (DMEM; Gibco, Grand Island, N.Y., USA) supplemented with 10% fetal calf serum (FCS; Gibco), 80 IU/ml penicillin and 80 µg/ml streptomycin (Sigma-Aldrich, Dorset, UK).

Chemicals and solutions

Specific monoclonal antibodies for MLC were purchased from Sigma-Aldrich. The secondary antibody, goat anti-mouse IgG conjugated to horseradish peroxidase was obtained from New England Biolabs (Hitchin, Herts., UK). ML-7, a specific inhibitor for MLCK, was purchased from Calbiochem (CN Biosciences, Nottingham, UK). $MLCK_{(11–19)}$ amide, an inhibitory peptide for MLCK, was purchased from Alexis (Nottingham, UK). This compound is a substrate-specific inhibitor of MLCK and corresponds to the region around the phosphorylation site (i.e. Ser^{19}) of MLC from chicken gizzard with the sequence: Lys^{11}-Lys^{12}-Arg^{13}-Ala^{14}-Ala^{15}-Arg^{16}-Ala^{17}-Thr^{18}-Ser^{19}. Two substitutions were made in that Pro^{14} and Gln^{15} were replaced with Ala. This improves the inhibitory potency of the synthetic peptide [21]. All other chemicals were obtained from Sigma-Aldrich. The osmolarity of solutions was monitored using a vapour pressure osmometer (Wescor 5500, Schlag, Gladbach, Germany). The isotonic medium (300±3 mosm l^{-1}) contained (in mM): NaCl 100, KCl 5, $MgCl_2$ 1, $CaCl_2$ 1.5, glucose 10, HEPES 10 and mannitol 70, titrated to pH 7.4 with NaOH. The components of the hypotonic medium were the same as those of the isotonic medium except that mannitol was omitted, resulting in a 23% hypotonicity (230±3 mosm l^{-1}). In the experiments of in which extracellular $[Ca^{2+}]$, the 1.5 mM $CaCl_2$ was omitted from the bath solution and 1.5 mM EGTA added. To measure the activity of the swelling-activated Cl^- channel, KCl was replaced by CsCl in the media and the pipette solutions contained (in mM): CsCl 40, Cs-aspartate 100, $MgCl_2$ 1, $CaCl_2$ 1.93, EGTA 5, ATP 2, GTP 0.5, HEPES 5. In this pipette solution, the free $[Ca^{2+}]$ was buffered at 100 nM. In some experiments, the free $[Ca^{2+}]$ was buffered to near zero by the following components of pipette solution (in mM): CsCl 40, Cs-aspartate 100, $MgCl_2$ 1, BAPTA 10, ATP 2, GTP 0.5, HEPES 5. To activate the Cl^- current directly by high intracellular Ca^{2+}, pipette solutions were used in which the free $[Ca^{2+}]$ was adjusted to 100, 250, 500 or 1000 nM by adding appropriate amounts of $CaCl_2$ to the pipette solution, as estimated with EQCAL software. All pipette solutions were adjusted to pH 7.2 with CsOH. The solvent for certain chemicals was DMSO, the final concentration of which in all experiments was less than 0.05%. This DMSO concentration had no effect on electrophysiological recordings, flux, calcium and protein measurements.

Fluorescence measurements of $[Ca^{2+}]_i$ with fura-2

$[Ca^{2+}]_i$ was measured with the fura-2 fluorescence ratio method on a fluorimeter (F-2000 spectrophotometer, Hitachi, Tokyo, Japan) as previously described [22]. In brief, cells attached on a cover-slip were loaded with 2 µM fura-2/acetoxymethyl ester (fura-2/AM) in DMEM culture medium at room temperature for 40 min and then at 37 °C for 20 min. After loading, cells were washed 3 times with PBS. After washing, the cover-slip was mounted in a custom-made holder and placed in a 5-ml quartz cuvette. Fluorescence emission was collected from a group of approximately 10^5 cells located in the excitation path. Excitation wavelength was alternated between 340 and 380 nm and fluorescence intensity ($F340$ and $F380$ respectively) was monitored at 510 nm. $[Ca^{2+}]_i$ was expressed as the ratio $F340/F380$ ratio, an indicator of Ca^{2+} activity [23].

Electrophysiological measurements

The whole-cell mode of the patch-clamp technique was used to measure membrane currents at room temperature (22–25 °C) as previously described [9, 12]. When the pipettes were connected to the input stage of an amplifier (Axopatch-200A, Axon Instruments, Union City, Calif., USA), their DC resistance was 3–5 MΩ. A Ag-AgCl wire was used as reference electrode. The current/voltage (I/V) relationship and time course of swelling-activated Cl^- current were obtained from either a ramp or a step protocol. The ramp protocol consisted of a step to –80 mV for 0.4 s followed by a 1.3-s linear voltage ramp to +80 mV, after which the potential was stepped back to the holding potential of –20 mV. This protocol was repeated every 15 s from a holding potential of –20 mV. Currents were sampled at 2-ms intervals (1024 points per record, filtered at 200 Hz). The step protocol consisted of a 1-s voltage step applied every 15 s from a holding potential of –20 mV to test potentials from –80 to +80 mV or +120 mV with an increment of 20 mV. Currents were sampled at 1-ms intervals. The normalized hypotonicity-induced current was used to compare the VSOAC activity in various experimental conditions. It was defined as the difference in current density between isotonic and hypotonic solutions and expressed per unit membrane capacitance. Cell capacitance was 23±1.7 pF (n=82) in this study. Data from electrophysiological experiments were digitized and analysed using pCLAMP software (v. 6.0.3, Axon Instruments).

Functional [^{3}H]taurine efflux assays

[^{3}H]Taurine efflux experiments were carried out at room temperature as described in detail elsewhere [24]. In brief, SiHa cells grown on six-well plates were pre-incubated with isotonic culture medium loaded with 1 µCi ml^{-1} [^{3}H]taurine (NEN Life Science Products, Boston, Mass., USA) for 2 h at 37 °C. After pre-incubation, the loading medium was aspirated and the cells washed rapidly 7 times with PBS. After washing, appropriate efflux medium with or without the drugs to be tested was added to the cells for a 15-min preincubation at room temperature. After preincubation, 1-ml aliquots of efflux medium were taken and replaced at indicated intervals and saved for counting. The drugs tested were present throughout the preincubation and flux measurement periods. Release of [^{3}H]taurine from preloaded cells was measured from the efflux medium at indicated intervals within a 25 min duration. Cells were finally lysed with 0.5 M NaOH to release the remaining [^{3}H]taurine. The radioactivity present in the efflux samples and in cell lysates was then determined by liquid scintillation counting. [^{3}H]Taurine efflux rate constants were estimated from

the negative slope of the graph of $\ln[X_i(t)/X_i(t=0)]$ vs. time (t), where $X_i(t=0)$ denotes the total amount of [^{3}H]taurine inside the cells at the beginning of the efflux time course and $X_i(t)$ the amount of [^{3}H]taurine inside the cells at time t. Following hypotonic shock, [^{3}H]taurine efflux occurs in two phases: an initial fast loss within 5 minutes and a slower subsequent loss [10]. The [^{3}H]taurine efflux rate constant in the hypotonic solution was therefore calculated from the negative slope of the semi-logarithm graph in the initial 5 min after exposure to hypotonicity. The swelling-activated [^{3}H]taurine efflux was defined as the difference between the efflux rate constants in hypotonic and isotonic solutions.

Determination of MLC phosphorylation

SiHa cells grown in 100-mm dishes to 90% confluence were washed 3 times with serum- and PO_4-free DMEM and labelled metabolically for 3 h at 37 °C with 250 µCi ml^{-1} [^{32}P]orthophosphate (NEN Life Science Products) in PO_4-free DMEM supplemented with 10% FCS. Before experiments, the cells were left at room temperature for 1 h and the cell culture then washed with PBS and replaced by isotonic or hypotonic solution. After stimulation with hypotonic solution, cells were washed quickly with ice-cold PBS and harvested on ice with protein lysis solution containing a protease inhibitor cocktail (Roche Diagnostic) (in mM): 100 KCl, 80 NaF, 10 EGTA, 50 β-glycerophosphate, 10 *p*-nitrophenyl phosphate, 1 vanadate, 0.5% sodium deoxycholate, 1% Nonidet P-40. Lysates were collected and microcentrifuged for 5 min at 4 °C. Protein concentrations were determined with a Bio-Rad protein assay. Equal amounts of proteins were separated by 12% SDS-polyacrylamide gel electrophoresis (SDS-PAGE) then transferred to polyvinylidene difluoride membranes (PVDF; Stratagene, La Jolla, Calif., USA). The MLC phosphorylation was detected by autoradiography. To identify the MLC position in the autoradiograph, the same PVDF membrane was immunoblotted with monoclonal MLC antibody using the following procedure. Non-specific binding was blocked with 5% (w/v) non-fat dried milk in PBS overnight at 4 °C. The blots were incubated with monoclonal MLC antibody at 1/5000 dilution in PBS with 0.1% Tween for 2 h at 37 °C, washed with PBS 4 times (10 min/each time) and then incubated with goat anti-mouse IgG conjugated to horseradish peroxidase at 1/5000 dilution for 1 h at room temperature. Following washing, the membrane was developed with enhanced chemiluminescence reagents according to the manufacturer's instructions (Amersham Pharmacia Biotech, Bucks, UK).

Statistics

All values in the present study are reported as means±SEM. Student's *t*-test for paired or unpaired samples was used for statistical analyses. Differences between values were considered significant when $P<0.05$. The concentration/inhibition curves for the drug effects were fitted to the following equation:

$$\%\text{inhibition} = \frac{100}{1+\left(\frac{IC_{50}}{C}\right)^{P}}$$

where C is the drug concentration, P the Hill coefficient and IC_{50} the drug concentration needed for half-maximal inhibition.

Results

MLCK inhibitors attenuate hypotonicity-induced Ca^{2+} signalling

The Ca^{2+} signalling in response to hypotonicity was investigated in SiHa cells loaded with the Ca^{2+}-sensitive dye fura-2/AM. Superfusion with a hypotonic solution (230 mosm l^{-1}) resulted in a rapid increase of the fluorescence ratio, from a basal level of 1.77±0.01 to a peak of 2.35±0.04 ($P<0.01$; $n=12$). The initial steep rise of $[Ca^{2+}]_i$ was followed by a decay to a plateau of 1.90±0.03 (Fig. 1A, B). To explore the possibility that MLCK may be involved in the regulation of hypotonicity-induced Ca^{2+} signalling, the effects of ML-7 and $MLCK_{(11–19)}$ amide, two structurally unrelated, mem-

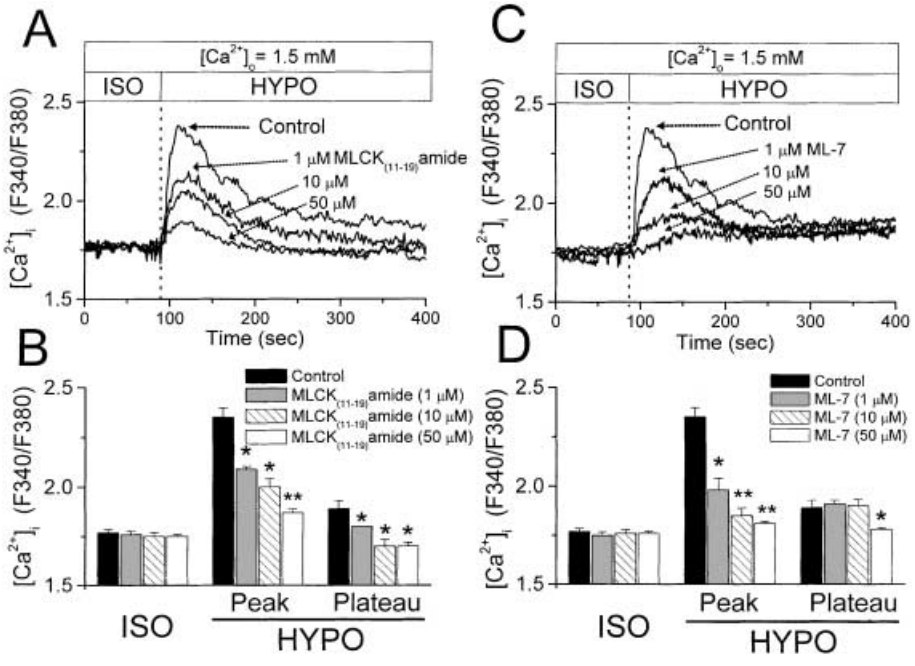

Fig. 1A–D Myosin light chain kinase (MLCK) inhibitors concentration-dependently attenuate Ca^{2+} signalling in swollen cervical cancer (SiHa) cells. **A**, **C** Representative recordings of the changes of intracellular $[Ca^{2+}]$ ($[Ca^{2+}]_i$) evoked by replacing the isotonic (*ISO*, 300 mosm l^{-1}) bathing medium by a hypotonic solution (*HYPO*, 230 mosml^{-1}) containing 1.5 mM Ca^{2+} ($[Ca^{2+}]_o$). SiHa cells were pre-incubated with 0.05% DMSO (*Control*) or MLCK inhibitors ($MLCK_{(11–19)}$ *amide* and *ML-7*) for 15 min at room temperature before $[Ca^{2+}]_i$ measurement. The drugs were also present during $[Ca^{2+}]_i$ measurement. **B**, **D** Summary of the changes of $[Ca^{2+}]_i$ evoked by hypotonicity. Means±SEM, $n=12$. *$P<0.05$, **$P<0.01$ vs. control, unpaired *t*-test

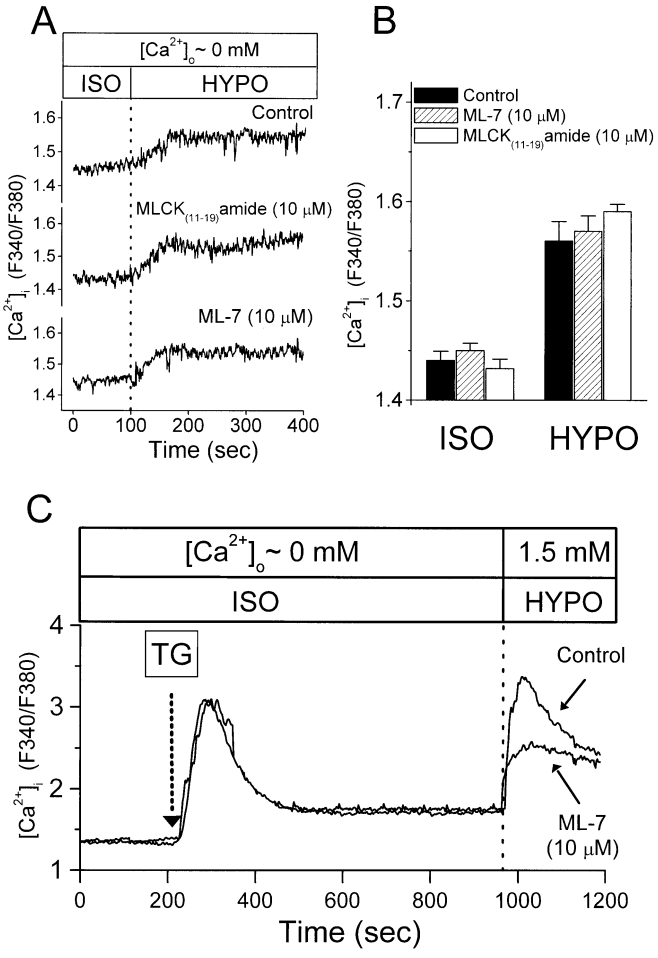

Fig. 2A–C MLCK mediates Ca^{2+} entry in response to hypotonicity. **A** A recording representative of ten different experiments showing the changes of $[Ca^{2+}]_i$ evoked by hypotonic solution in the absence of extracellular Ca^{2+}, plus 1.5 mM EGTA *($[Ca^{2+}]_o$ ~0 mM*). **B** Summary of hypotonicity-induced Ca^{2+} signalling in the absence of $[Ca^{2+}]_o$. Means±SEM, n=10. **C** Representative recordings showing the effect of 2 μM thapsigargin (*TG*) on $[Ca^{2+}]_i$ in the absence or presence of $[Ca^{2+}]_o$. SiHa cells were pre-incubated with 0.05% DMSO (*Control*) or drugs for 15 min at room temperature before $[Ca^{2+}]_i$ measurement. The drugs tested were also present during $[Ca^{2+}]_i$ measurement

brane-permeable, potent and specific inhibitors of MLCK, on Ca^{2+} signalling were investigated. $MLCK_{(11–19)}$ amide is a substrate-specific inhibitory peptide of MLCK and corresponds to the region around the phosphorylation site of MLC [21]. ML-7, a synthetic napthalenesulphonyl compound, blocks ATP binding to MLCK [25]. Whilst cell treatment with ML-7 or $MLCK_{(11–19)}$ amide did not affect the basal level of $[Ca^{2+}]_i$, both attenuated the hypotonicity-stimulated increase of $[Ca^{2+}]_i$ concentration dependently (Fig. 1). $MLCK_{(11–19)}$ amide (1 μM) inhibited the peak rise of the fluorescence ratio from 2.35±0.04 to 2.09±0.01 (P<0.05, n=12) and also significantly suppressed the plateau level after hypotonic exposure (control: 1.90±0.03 vs. $MLCK_{(11–19)}$ amide: 1.79±0.003). Higher concentrations of $MLCK_{(11–19)}$ amide (10 and 50 μM) further decreased the peak level to 2.00±0.03 (n=12) and 1.87±0.015 (n=12), respectively, and also depressed the plateau level significantly. ML-7 also inhibited the $[Ca^{2+}]_i$ rise evoked by hypotonicity concentration dependently (Fig. 1C, D). The IC_{50} values for the inhibition of the initial peak rise of $[Ca^{2+}]_i$ were 0.8 and 2.1 μM for ML-7 and $MLCK_{(11–19)}$ amide, respectively.

Subsequent experiments were done by altering extracellular $[Ca^{2+}]$ ($[Ca^{2+}]_o$). Figure 2 shows the effect of $MLCK_{(11–19)}$ amide and ML-7 on the hypotonicity-induced Ca^{2+} signalling with a $[Ca^{2+}]_o$ of practically 0 mM. Under this condition, hypotonic stress only induced a small, progressive increase of $[Ca^{2+}]_i$, from a basal level of 1.42±0.003 to a plateau of 1.59±0.006 (Fig. 2A, P<0.05; n=10), while neither $MLCK_{(11–19)}$ amide nor ML-7 affected this Ca^{2+} signalling. These findings indicate that $MLCK_{(11–19)}$ amide and ML-7 inhibited Ca^{2+} entry from the extracellular medium, but did not affect the mobilization of Ca^{2+} from intracellular stores.

To confirm the effect of MLCK on Ca^{2+} entry, 2 μM thapsigargin, an inhibitor of the Ca^{2+}-ATPase in the endoplasmic reticulum, was used to deplete the internal Ca^{2+} stores in the absence of $[Ca^{2+}]_o$. Cells were then exposed to a Ca^{2+}-containing hypotonic solution. As shown in Fig. 2C, pretreatment with 10 μM ML-7 significantly reduced the peak level of Ca^{2+} signalling induced by hypotonicity (control: 3.30±0.01 vs. ML-7: 2.45±0.005; n=5, P<0.01, unpaired t-test).

Ca^{2+} dependence of VSOAC activation

We studied the significance of Ca^{2+} signalling in volume regulation further. As shown in Fig. 3A, whole-cell voltage-clamp recordings were obtained from SiHa cells, in which the pipette solution contained 1.93 mM $CaCl_2$ and 5 mM EGTA with 1.5 mM $CaCl_2$ in the extracellular medium. Membrane currents recorded during the ramp protocol applied in isotonic solutions were small. Exposure to a hypotonic solution induced cell swelling and activated a large, outwardly rectifying current. When the pipette solution contained 10 mM BAPTA and there was no Ca^{2+} in the extracellular medium, more than 85% of VSOAC activity was suppressed (Fig. 3, control: 90±3 pA pF^{-1}, n=24 vs. Ca^{2+}-free: 12±2 pA pF^{-1}, n=10; P<0.01, unpaired t-test). This indicates that hypotonicity-induced Ca^{2+} signalling is important for the activation of VSOAC.

A question arises promptly: is it possible to activate VSOAC simply by increasing $[Ca^{2+}]_i$? To test this point, we loaded SiHa cells with a pipette solution buffered at an elevated $[Ca^{2+}]_i$. Figure 4A shows current traces recorded during the voltage-step protocol from cells loaded with different $[Ca^{2+}]_i$ and Fig. 4B shows the current densities at +120 and –80 mV as a function of $[Ca^{2+}]_i$. Increasing $[Ca^{2+}]_i$ stimulated a current with time-dependent activation at more positive potentials (>60 mV), which is a typical characteristic of the Ca^{2+}-activated Cl^- current [26]. In contrast, VSOAC showed time-depen-

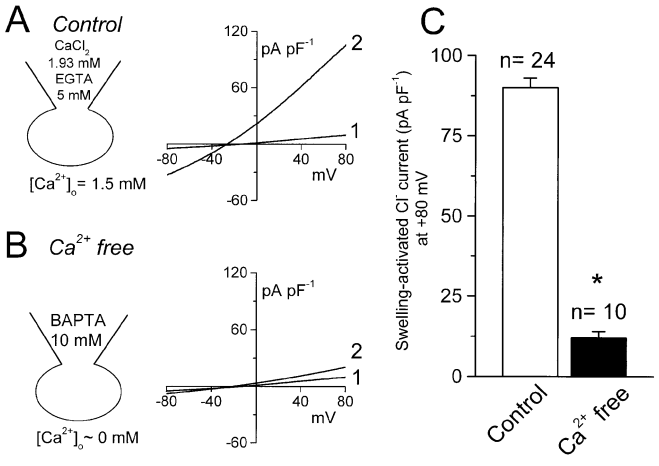

Fig. 3A–C The activation of swelling-activated Cl^- channels depends on Ca^{2+} signalling. **A** Representative current traces (ramp protocol) recorded under isotonic and hypotonic solutions with $[Ca^{2+}]_i$ buffered at 100 nM by 5 mM EGTA (Control). The perfusing isotonic or hypotonic solution contained 1.5 mM Ca^{2+} *($[Ca^{2+}]_o$=1.5 mM)*. **B** Current traces recorded in isotonic and hypotonic solutions with $[Ca^{2+}]_i$ buffered near 0 nM. For these experiments, the pipette solution contained 10 mM BAPTA and the external solution was free of Ca^{2+}, plus 1.5 mM EGTA *($[Ca^{2+}]_o$ ~0 mM)*. Trace *1*: basal membrane current recorded in the isotonic solution; trace *2*: currents recorded after perfusion with hypotonic solution. **C** Swelling-activated Cl^- currents measured at +80 mV in *n* cells. **P*<0.01, unpaired *t*-test

dent inactivation at more positive potentials (Fig. 4C). This suggests increasing $[Ca^{2+}]_i$ alone is not adequate to activate VSOAC.

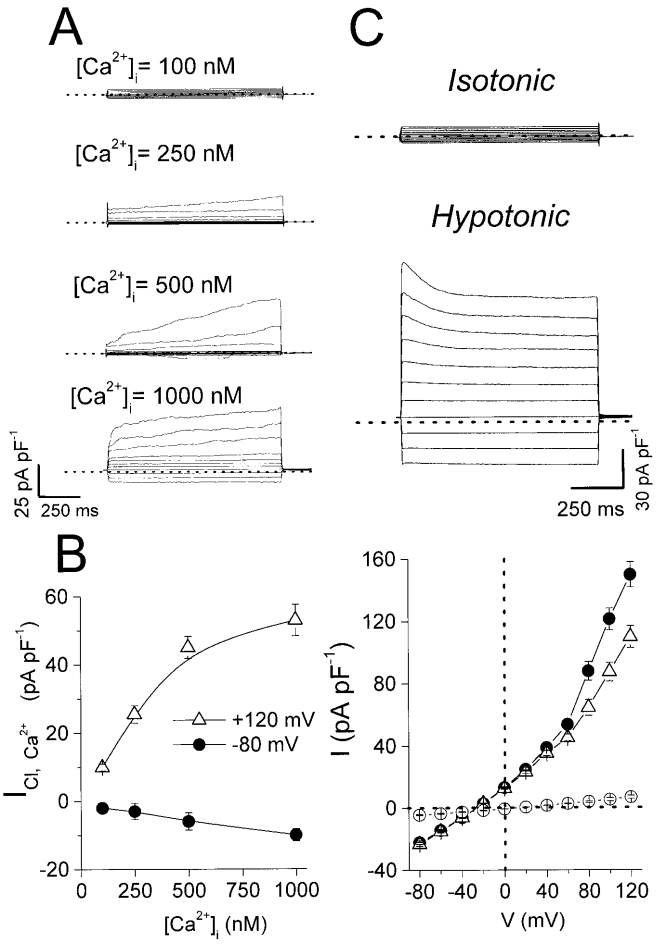

Fig. 4 **A** Representative current traces during voltage step protocol in cervical cancer SiHa cells loaded via the patch pipette with $[Ca^{2+}]_i$ buffered at 100, 250, 500 or 1000 nM. **B** Steady-state current/$[Ca^{2+}]_i$ relationship at +120 mV (*open triangles*) and –80 mV (*closed circles*). **C** Swelling-activated Cl^- currents in cervical cancer SiHa cells. Current traces (step protocol) recorded in isotonic and hypotonic solutions. *Horizontal lines* represent zero current levels. Current/voltage (*I*/*V*) relationships were obtained from traces in isotonic and hypotonic solutions. *Closed circles* and *open triangles* are the hypotonicity-induced current at the beginning and end of pulse respectively; *open circles* are the current in isotonic solution. The step protocol for **A** and **C** consisted of a 1-s voltage step, applied every 15 s from a holding potential of –20 mV to test potentials from –80 to +120 mV with an increment of 20 mV. Means±SEM, *n*=5

The activation of VSOAC requires MLCK activity

To study the significance of MLCK activity in volume regulation, whole-cell voltage-clamp recordings were obtained from SiHa cells. Membrane currents recorded during the step protocol applied to SiHa cells in isotonic solutions were small and independent of time (Fig. 5A). Exposure to a hypotonic solution (230 mosm l^{-1}) induced cell swelling and activated a large, outwardly rectifying current. At potentials more positive than +60 mV, the currents showed time-dependent inactivation; this became more pronounced at higher membrane potentials (Fig. 5A). Intracellular dialysis with $MLCK_{(11–19)}$ amide markedly and concentration-dependently reduced the activity of the volume-regulated Cl^- channel (Fig. 5). For control cells, the swelling-activated Cl^- current was 90±3 pA pF^{-1} (*n*=24) at +80 mV. The current density decreased significantly to 65±4 (*n*=6), 38±3 (*n*=12) and 18±5 (*n*=6) pA pF^{-1} with 1, 10 and 50 μM $MLCK_{(11–19)}$ amide, respectively (Fig. 5B). The other MLCK inhibitor, ML-7, had similar effects on the activity of the volume-regulated Cl^- channel. As depicted in Fig. 6, intracellular dialysis with ML-7 did not change the isotonic Cl^- current (trace 1), but inhibited the activation of the volume-regulated Cl^- channel concentration dependently. For the inhibition of swelling-activated Cl^- current, IC_{50} values were 10.4 and 6.0 μM for ML-7 and $MLCK_{(11–19)}$ amide, respectively.

In addition to altering the current amplitude, the activation rate of the volume-regulated Cl^- channel was also significantly decreased by ML-7 and $MLCK_{(11–19)}$ amide (Fig. 7). In the control group, exposure to hypotonicity activated the outwardly rectifying current rapidly (1.20±0.03 pA pF^{-1} s^{-1} at +80 mV, *n*=24). The rate of current activation was significantly slower in ML-7- or $MLCK_{(11–19)}$ amide-treated cells: 0.51±0.05, *n*=12 and 0.34±0.02 pA pF^{-1} s^{-1}, *n*=12, respectively.

Hypotonicity-induced taurine transport also required MLCK activity. Figure 8 shows the time course of taurine

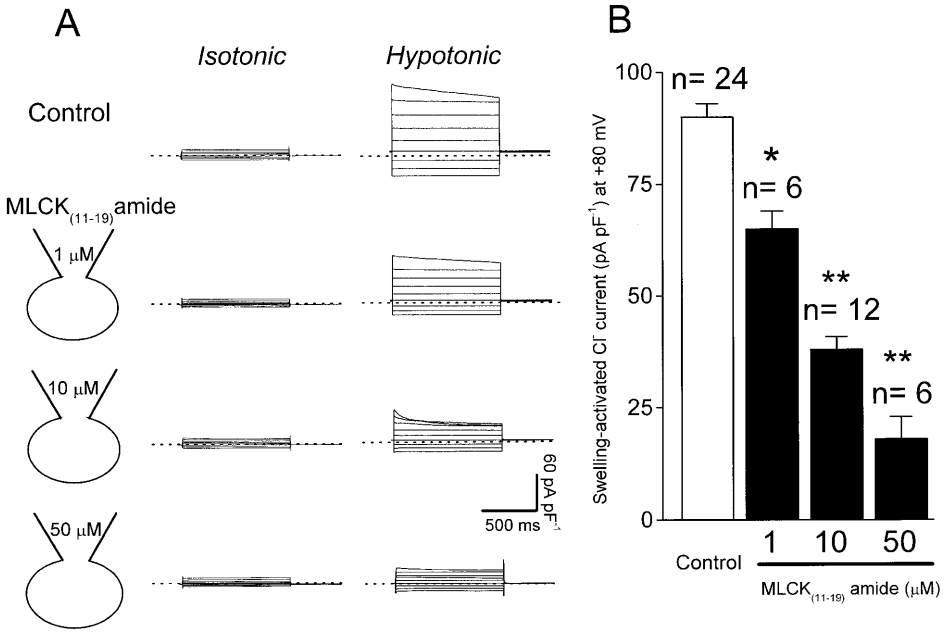

Fig. 5A, B $MLCK_{(11–19)}$ amide inhibited the activation of the swelling-activated Cl^- current concentration dependently. **A** Representative current traces (step protocol) recorded in isotonic and hypotonic solutions without (*Control*) or with intracellular dialysis with 1, 10 or 50 μM $MLCK_{(11–19)}$ amide. The *dotted line* is the zero current level. **B** Swelling-activated Cl^- currents measured at +80 mV in *n* cells. **P*<0.05, ***P*<0.01, unpaired *t*-test

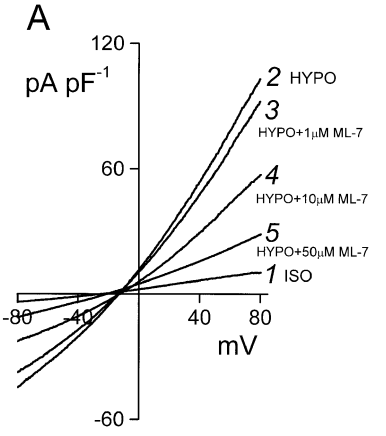

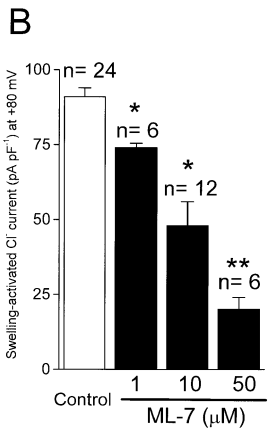

Fig. 6A, B ML-7 inhibited the activation of the swelling-activated Cl^- current concentration dependently. **A** Representative current traces (ramp protocol) recorded in isotonic and hypotonic solutions without (*Control*) or with intracellular dialysis with 1, 10 or 50 μM ML-7. Trace *1*: basal membrane current recorded under isotonic conditions for control cells and cells dialysed with ML-7; Trace *2*: currents recorded in control cells after perfusion with hypotonic solution; Traces *3–5*: hypotonic current recorded in cells dialysed with 1, 10 or 50 μM ML-7, respectively. **B** Swelling-activated Cl^- currents measured at +80 mV in *n* cells. **P*<0.05, ***P*<0.01, unpaired *t*-test

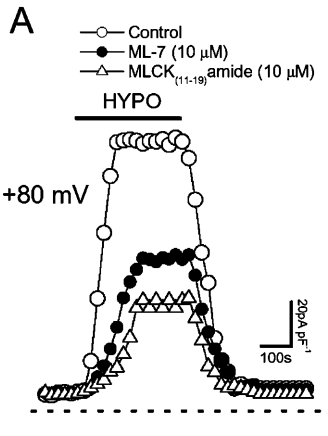

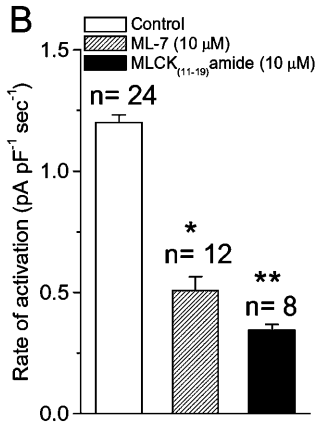

Fig. 7A, B Activation rate of the swelling-activated Cl^- channel was significantly decreased by ML-7 and $MLCK_{(11–19)}$ amide. **A** Time course of membrane currents activated at +80 mV in control cells or in cells after intracellular dialysis with 10 μM ML-7 or $MLCK_{(11–19)}$ amide. Data were obtained from the voltage ramp protocol applied every 15 s. *Thick horizontal bar*: application of hypotonic solution (230 mosm l^{-1}). *Horizontal dashed line*: zero current level. **B** Summary of activation rate for swelling-activated Cl^- channel under various conditions for *n* cells. **P*<0.05, ***P*<0.01, unpaired *t*-test

efflux from SiHa cells in the presence or absence of MLCK inhibitors. Efflux in isotonic medium was low and stable both in the presence or absence of MLCK inhibitors. Exposure to the hypotonic solution markedly increased the taurine efflux rate constant from 0.0095±0.002 to 0.19±0.01 min^{-1} (Fig. 8A, *P*<0.01, *n*=4). Cell pretreatment with 10 μM ML-7 or $MLCK_{(11–19)}$ amide for 15 min decreased the swelling-activated taurine efflux rate significantly by 55% and 79%, respectively (Fig. 8A and B). For $MLCK_{(11–19)}$ amide, the estimated IC_{50} and Hill coefficient were 2.0±0.2 μM (*n*=4) and 0.9±0.1 (*n*=4) respectively. In the case of ML-7, these values were 6.4±0.2 μM (*n*=4) and 0.8±0.1 (*n*=4) (Fig. 8C).

MLCK-mediated phosphorylation of MLC in response to hypotonic shock

Phosphorylation of MLC plays a key role in promoting cell contractility and shape in vertebrate muscle and non-

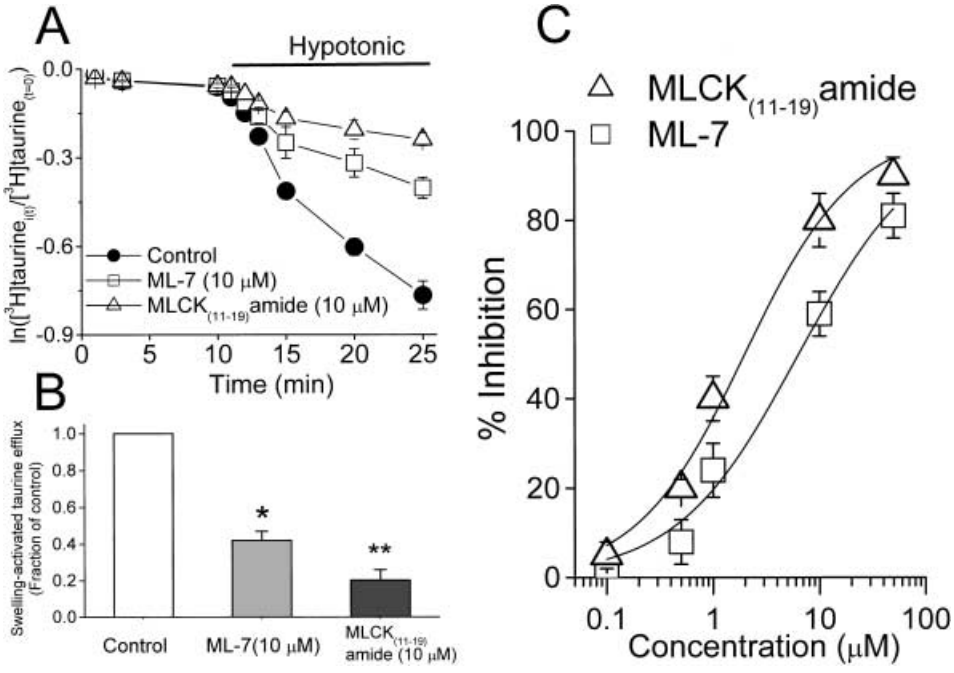

Fig. 8A–C Effect of MLCK inhibitors on swelling-activated taurine transport in human cervical cancer SiHa cells. **A** Time course of taurine efflux from SiHa cells exposed to isotonic and hypotonic media. The graph shows the logarithm of the fraction of the original intracellular [^{3}H]taurine remaining as a function of time. The *thick horizontal line* indicates the application of hypotonic solution (230 mosm l^{-1}). SiHa cells were pre-incubated with 0.05% DMSO (*Control*) or MLCK inhibitors [10 μM ML-7 or $MLCK_{(11–19)}$ amide] for 15 min at room temperature and then exposed to flux medium in the presence or absence of inhibitors. Means±SEM, n=4. **B** Summary of swelling-activated [^{3}H]taurine efflux rates, expressed as a fraction of control, under various conditions. Means±SEM, n=4. *P<0.05, **P<0.01 vs. control, unpaired t-test. **C** Concentration/response curves for the inhibition of swelling-activated taurine transport by ML-7 or $MLCK_{(11–19)}$ amide. Means±SEM, n=4

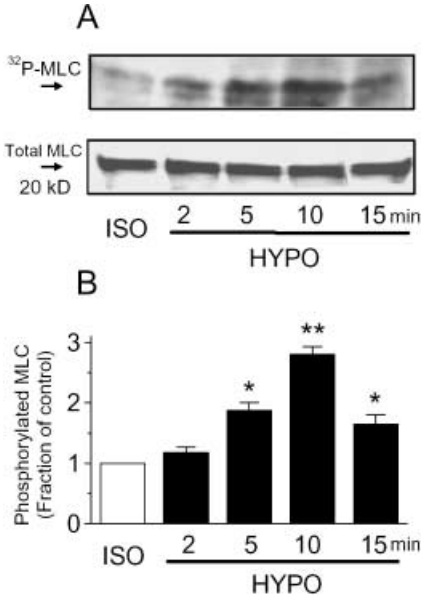

Fig. 9A, B Hypotonicity-induced MLC phosphorylation in cervical cancer SiHa cells. **A** Time courses of MLC phosphorylation in response to hypotonicity. *Total MLC*: MLC determined by immunoblotting; *^{32}P-MLC*: phosphorylated MLC determined by autoradiography after labelling with [^{32}P]orthophosphate (see Materials and methods). **B** Phosphorylated MLC measured by densitometry. Means±SEM, n=3 independent experiments. *P<0.05, **P<0.01 vs. isotonic, unpaired t-test

muscle cells. The molecular weight of MLC is approximately 20 kD. For cervical cancer cells, on a 12% SDS-PAGE, few proteins in the 26–20 kD range co-migrate with MLCK. To determine MLC phosphorylation, SiHa cells were labelled metabolically with [^{32}P]orthophosphate and exposed to isotonic or hypotonic solutions. Whole-cell extracts were then separated by 12% SDS-PAGE (50 μg/lane), transferred to PVDF, autoradiographed (^{32}P-MLC) and immunoblotted with monoclonal MLC antibody. As shown in Fig. 9, hypotonic shock significantly increased MLC phosphorylation, an effect which appeared after 5 min (87±14% increase) of hypotonic stimulation and reached a maximum (180±13% increase) at about 10 min. The total amount of MLC was constant and not affected by osmotic change (Fig. 9A).

The increased phosphorylation of MLC could have resulted from activation of MLCK or inhibition of MLC phosphatase [13]. We investigated further whether MLCK mediates the hypotonicity-induced phosphorylation of MLC. As shown in Fig. 10A and B, pre-treatment with 1 μM ML-7 completely abolished the hypotonicity-induced phosphorylation of MLC, indicating that the phosphorylation of MLC in response to hypotonicity is totally dependent on the activity of MLCK (Fig. 10A and B). Depletion of $[Ca^{2+}]_o$ also reduced the phosphorylation of MLC significantly, suggesting that MLCK-mediated phosphorylation of MLC requires Ca^{2+} entry (Fig. 10A and B).

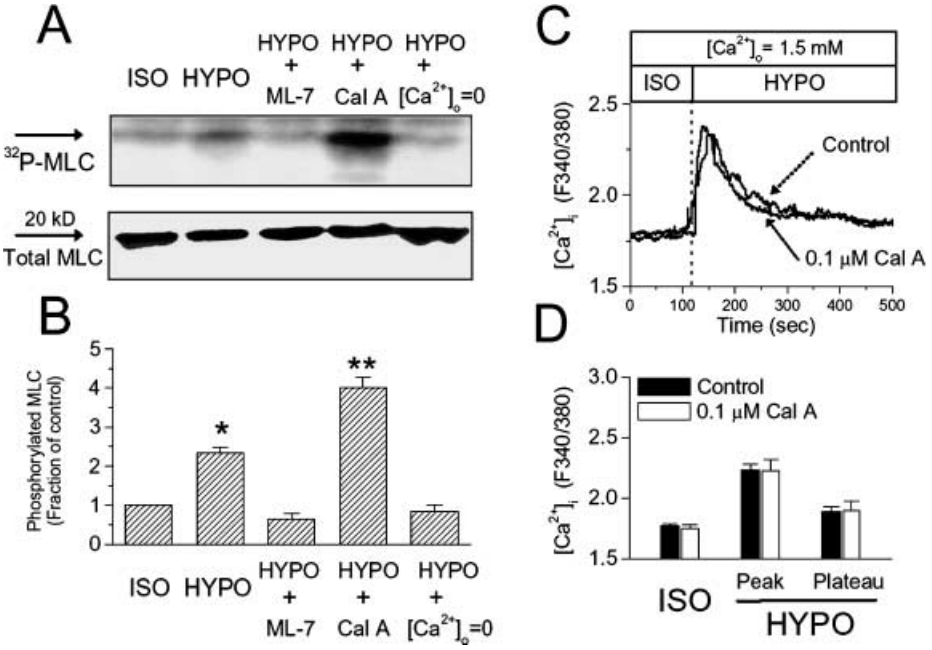

Fig. 10 **A**, **B** MLC phosphorylation in response to hypotonicity is mediated by MLCK activity and Ca^{2+} influx and is enhanced by calyculin A. MLC phosphorylation was determined 10 min after exposure to isotonic (300 mosm l^{-1}) or hypotonic (230 mosm l^{-1}) solution. ML-7 (1 μM), calyculin A (0.1 μM), or 0 mM $[Ca^{2+}]_o$ plus 1.5 mM EGTA ($[Ca^{2+}]_o=0$), was applied 15 min before and during stimulation with hypotonic stress. MLC phosphorylation was determined as described in Materials and methods. Means±SEM, n=3 independent experiments. *P<0.05, **P<0.01 vs. isotonic, unpaired t-test. **C**, **D** No effect of calyculin A (0.1 μM) on Ca^{2+} signalling in response to hypotonicity. SiHa cells were pre-incubated with 0.05% DMSO (*Control*) or calyculin A (*Cal A*, 0.1 μM) for 15 min at room temperature before $[Ca^{2+}]_i$ measurement. The drug tested was also present during $[Ca^{2+}]_i$ measurement. Means±SEM, n=6

However, it remained unclear whether MLCK regulated Ca^{2+} entry by acting directly on Ca^{2+} influx pathways or indirectly through MLC phosphorylation. Accordingly, calyculin A, an inhibitor of types-1 and -2A phosphatase [27], was used to enhance MLC phosphorylation and therefore investigate its effect on hypotonicity-induced Ca^{2+} signalling. As shown in Fig. 10A and B, 0.1 μM calyculin A further increased the phosphorylated form of MLC induced by hypotonicity but had no effect on the Ca^{2+} signalling in response to hypotonic shock (Fig. 10C and D). This suggests that MLCK controls Ca^{2+} signalling via by an MLC phosphorylation-independent mechanism.

Discussion

This study demonstrates the involvement of MLCK in the volume regulation of human cervical cancer (SiHa) cells. Ca^{2+} entry in response to hypotonic stress was largely blocked by the inhibition of MLCK activity. ML-7 and $MLCK_{(11–19)}$ amide inhibited the hypotonicity-induced Ca^{2+} entry with IC_{50}s of 0.8 and 2.1 μM, respectively. These values are similar to reported inhibition constants of these inhibitors of MLCK in vitro (0.4 and 10 μM for ML-7 and $MLCK_{(11–19)}$ amide, respectively) [21, 25]. This suggests that MLCK is a modulator of Ca^{2+} entry during RVD. The amplitude and activation rate of VSOAC were also inhibited potently by blockers of MLCK, thereby identifying a functional link between MLCK activity and VSOAC activation. Activation of VSOAC correlates more closely with Ca^{2+} influx than with Ca^{2+} release from intracellular stores in human cervical cancer cells [8, 11, 12]. Here we also demonstrated that the activation of VSOAC depends on Ca^{2+} signalling. Accordingly, it is likely that a cause-effect relationship exists between the inhibitory effects exerted by blocking MLCK activity on Ca^{2+} entry and activation of VSOAC. In addition to regulating Ca^{2+} entry and VSOAC activation, MLCK also mediated MLC phosphorylation in response to hypotonic stress. Ca^{2+} entry is also required for the MLCK-mediated MLC phosphorylation.

This result prompts the question of whether MLC phosphorylation is linked to the regulation of Ca^{2+} signalling in swollen cervical cancer cells. Several observations suggest a negative answer. First, 1 μM ML-7 inhibited only 50–60% of the Ca^{2+} transient in response to hypotonicity (Fig. 1) but completely abolished the hypotonicity-induced phosphorylation of MLC (Fig. 10). This indicates that MLC phosphorylation is not critically involved in the regulation of Ca^{2+} signalling. Second, enhancing phosphorylation of MLC by calyculin A had no effect on Ca^{2+} signalling and, further, the hypotonicity-induced MLC phosphorylation was itself dependent on Ca^{2+} entry from the extracellular medium. It is likely that MLCK regulates Ca^{2+} entry independently of MLC phosphorylation and that the MLCK-mediated Ca^{2+} entry in turn controls MLC phosphorylation. Third, hypotonicity-induced Ca^{2+} signalling showed a fast time

course in which $[Ca^{2+}]_i$ rose to a peak level at about 50 s and finally plateaued within 200 s on exposure to hypotonic stress. In contrast, hypotonicity-induced phosphorylation of MLC required 5 min to become significantly different on exposure to hypotonicity. The lack of consistency in these time courses rules out involvement of MLC phosphorylation in the regulation of hypotonicity-induced Ca^{2+} signalling. MLCK is known to regulate many contractile events in both muscle and non-muscle cells and therefore it is possible that the blockade of MLCK activity prevents cytoskeletal reorganization impinging on the Ca^{2+} influx pathways and thus secondarily modulates Ca^{2+} entry or production of another second messenger that activates Ca^{2+} activity [19, 28]. In addition to MLC, MLCK might phosphorylate other targets in swollen cervical cancer cells.

We have demonstrated recently that the functional integrity of actin filaments plays an essential role in maintaining the normal RVD responses and the activation of VSOAC in human cervical cancer cells [29]. Phosphorylation of MLC can promote the contraction of the actin-based cytoskeleton. Therefore, there is a possible linkage between MLC phosphorylation and RVD. It is likely that hypotonic stress changes cytoskeletal dynamics by increasing MLCK activity and subsequent MLC phosphorylation. However, it is important to establish whether MLC phosphorylation directly triggers the activation of VSOAC. In fact, this is not so for the following reasons. First, Ca^{2+} signalling is critical for the activation of VSOAC (Fig. 3), but MLC phosphorylation does not control this Ca^{2+} signalling. Second, 1 μM ML-7 inhibited activation of VSOAC to a minor extent, but completely abolished the hypotonicity-induced MLC phosphorylation, implying that MLC phosphorylation is not critically involved in the regulation of VSOAC. Third, thrombin increases MLC phosphorylation by inhibiting MLC phosphatase [30] but does not activate VSOAC in endothelial cells under isotonic conditions [31]. Similarly, the nuclear inhibitor of protein phosphatase-1 [NIPP-1(191–210)], an inhibitory peptide for MLC phosphatase, has no effect on membrane current under isotonic conditions [32].

MLCK activity is reportedly involved in activating ion currents in some cell types. For example, there is a positive correlation between MLCK activity and VSOAC activation in calf pulmonary artery endothelial cells [32]. MLCK could also mediate the noradrenaline-evoked cation current in rabbit portal vein myocytes [17]. In bullfrog sympathetic neurons, inhibiting MLCK activity reduces the amplitude of voltage-dependent K^+ currents [33] and the carbachol-activated non-selective cation currents in guinea-pig gastric myocytes are modulated by MLCK activity [16]. In spite of these examples, it is not established how MLCK activity or MLC phosphorylation regulates the activities of these ion channels.

Here we demonstrate that the activation of VSOAC depends on the hypotonicity-induced $[Ca^{2+}]_i$ transient. This result is consistent with our previous findings in another cervical cancer cell line (HT-3 cells) indicating that activation of a volume-sensitive Cl^- channel requires Ca^{2+} entry [12]. However, simply increasing $[Ca^{2+}]_i$ could not activate VSOAC. In swollen cervical cancer cells, several signal pathways are activated, such as protein kinase Cα (PKCα) and extracellular-signal related kinase-1 (ERK1)/ERK2 mitogen-activated protein kinase (MAP kinase) pathway. The activation of PKCα and ERK1/ERK2 MAP kinase pathways requires Ca^{2+} entry and is critical for the activity of VSOAC [12, 34]. Accordingly, the activation of VSOAC involves the hypotonicity-induced Ca^{2+} transient coupled with other signalling pathways.

Osmotic swelling of SiHa cells induces an initial steep rise of $[Ca^{2+}]_i$ that is followed by a decay to a plateau. The initial peak rise of $[Ca^{2+}]_i$ reflects the activation of Ca^{2+} entry across the cell membrane and the plateau level of $[Ca^{2+}]_i$ is mainly maintained by Ca^{2+} release from intracellular stores [34]. ML-7 and $MLCK_{(11–19)}$ amide seem not to act in the same manner on the hypotonicity-induced Ca^{2+} transient. In addition to inhibiting the peak rise of Ca^{2+} transient, $MLCK_{(11–19)}$ amide depressed the plateau. This indicates $MLCK_{(11–19)}$ amide might inhibit the internal release of Ca^{2+} as well.

The common pathways for swelling-induced taurine transport and the volume-sensitive Cl^- channel are still being debated. In cervical cancer cells, despite the lack of molecular identity, these two swelling-activated transport pathways share the same signal pathways, have similar sensitivities to Cl^- channel inhibitors [e.g. 5-nitro-2-(3-phenylpropylamino)benzoate (NPPB) and tamoxifen] and are modulated by hypotonicity-induced Ca^{2+} transient [34]. Here we show that the activation of volume-regulated Cl^- channel is concentration-dependently inhibited by ML-7 and $MLCK_{(11–19)}$ amide with IC_{50}s of 10.4 and 6.0 μM, respectively. For swelling-activated taurine transport, the IC_{50}s were 6.4 and 2.0 μM, respectively. These values are not considerably different.

The present study demonstrates that MLCK has a novel function, namely to regulate the activation of VSOAC by mediating Ca^{2+} entry in response to hypotonicity. This novel function of MLCK in Ca^{2+} signalling does not correlate with MLC phosphorylation. We therefore propose that, in addition to MLC, MLCK might phosphorylate other targets or have other immediate downstream substrates in swollen cervical cancer cells. The most likely target is the Ca^{2+} channel that is responsible for hypotonicity-induced Ca^{2+} entry, or the signal pathway linked with the activation of Ca^{2+} channel. We are trying to identify the Ca^{2+} channel using both molecular and electrophysiological approaches. Until the molecular and electrophysiological identities of the Ca^{2+} channel and the underlying signal pathways are established, we are limited to indirect methods to show this unusual MLCK function in cervical cancer cells. Nevertheless, the use of structurally unrelated specific inhibitors allows us to make significant progress in demonstrating this novel role for MLCK.

Acknowledgements This work was partly supported by the Wellcome Trust and National Science Council, Taiwan (NSC 89-2314-B-006-0112 and NSC 90-2314-B-006-032). Meng-Ru Shen holds a Swire Scholarship supported by John Swire and Sons Ltd.

References

1. Kirk K (1997) Swelling-activated organic osmolyte channels. J Membr Biol 158:1–16
2. Okada Y (1997) Volume expansion-sensing outward-rectifier Cl^- channel: fresh start to the molecular identity and volume sensor. Am J Physiol 273:C755–C789
3. Nilius B, Eggermont J, Voets T, Buyse G, Manolopoulos V, Droogmans G (1997) Properties of volume-regulated anion channels in mammalian cells. Prog Biophys Mol Biol 68:69–119
4. Lang F, Busch GL, Ritter M, Völkl H, Waldegger S, Gulbins E, Haussinger D (1998) Functional significance of cell volume regulatory mechanisms. Physiol Rev 78:247–306
5. Chou CY, Shen MR, Wu SN (1995) Volume-sensitive chloride channels associated with human cervical carcinogenesis. Cancer Res 55:6077–6083
6. Chou CY, Shen MR, Chen TM, Huang KE (1997) Volume-activated taurine transport is differentially activated in human cervical cancer HT-3 cells, but not activated in HPV-immortalized Z 183A and normal cervical epithelial cells. Clin Exp Pharmacol Physiol 24:935–939
7. Shen MR, Wu SN, Chou CY (1996) Volume-sensitive chloride channels in the primary culture cells of human cervical carcinoma. Biochim Biophys Acta 1315:138–144
8. Shen MR, Chou CY, Wu ML, Huang KE (1998) Differential osmosensing signalling pathways and G-protein involvement in human cervical cells with different tumor potential. Cell Signal 10:113–120
9. Shen MR, Droogmans G, Eggermont J, Voets T, Ellory JC, Nilius B (2000) Differential expression of volume-regulated anion channels during cell cycle progression of human cervical cancer cells. J Physiol (Lond) 529:385–394
10. Shen MR, Chou CY, Ellory JC (2001) Swelling-activated taurine and K^+ transport in human cervical cancer cells: association with cell cycle progression. Pflugers Arch 441:787–795
11. Shen MR, Ellory JC (2001) Calcium signalling in regulatory volume decrease of human cervical cancer cells. J Physiol (Lond) 533:9P–10P
12. Chou CY, Shen MR, Hsu KS, Huang HY, Lin HC (1998) Involvement of PKC-α in regulatory volume decrease responses and activation of volume-sensitive chloride channels in human cervical cancer HT-3 cells. J Physiol (Lond) 512:435–448
13. Somlyo AP, Somlyo AV (1994) Signal transduction and regulation in smooth muscle. Nature 372:231–236
14. Sanders LC, Matsumura F, Bokoch GM, Lanerolle P de (1999) Inhibition of myosin light chain kinase by p21-activated kinase. Science 283:2083–2085
15. Nguyen DH, Catling AD, Webb DJ, Sankovic M, Walker LA, Somlyo AV, Weber MJ, Gonias SL (1999) Myosin light chain kinase functions downstream of Ras/ERK to promote migration of urokinase-type plasminogen activator-stimulated cells in an integrin-selective manner. J Cell Biol 146:149–164
16. Kim YC, Kim SJ, Kang TM, Suh SH, So I, Kim KW (1997) Effects of myosin light chain kinase inhibitors on carbachol-activated nonselective cationic current in guinea-pig gastric myocytes. Pflugers Arch 434:346–353
17. Aromolaran AS, Albert AP Large WA (2000) Evidence for myosin light chain kinase mediating noradrenaline-evoked cation current in rabbit portal vein myocytes. J Physiol (Lond) 524:853–863
18. Watanabe H, Takahashi R, Zhang XX, Goto Y, Hayashi H, Ando J, Isshiki M, Seto M, Hidaka H, Niki I, Ohno R (1998) An essential role of myosin light-chain kinase in the regulation of agonist- and fluid flow-stimulated Ca^{2+} influx in endothelial cells. FASEB J 12:341–348
19. Wantanabe H, Tran QK, Takeuchi K, Fukao M, Liu MY, Kanno M, Hayashi T, Iguchi A, Seto M, Ohashi K (2001) Myosin light-chain kinase regulates endothelial calcium entry and endothelium-dependent vasodilation FASEB J 15:282–284
20. Nakao M, Ono K, Fujisawa S, Iijima T (1999) Mechanical stress-induced Ca^{2+} entry and Cl^- current in cultured human aortic endothelial cells. Am J Physiol 276:C238–C249
21. Pearson RB, Misconi LY, Kemp BE (1986) Smooth muscle myosin kinase requires residues on the COOH-terminal side of the phosphorylation site. J Biol Chem 261:25–27
22. Chen Y, Simasko SM, Niggel J, Sigurdson WJ, Sachs F (1996) Ca^{2+} uptake in GH3 cells during hypotonic swelling: the sensory role of stretch-activated ion channels. Am J Physiol 270:C1790–C1798
23. Grynkiewicz G, Poenie M, Tsien RY (1985) A new generation of Ca^{2+} indicators with greatly improved fluorescence properties. J Biol Chem 260:3440–3450
24. Shen MR, Chou CY, Ellory JC (2000) Volume-sensitive KCl cotransport associated with human cervical carcinogenesis. Pflugers Arch 440:751–760
25. Saitoh M, Ishikawa T, Matsushima S, Naka M, Hidaka H (1987) Selective inhibition of catalytic activity of smooth muscle myosin light chain kinase. J Biol Chem 262:7796–7801
26. Nilius B, Prenen J, Voets T, Bremt KVD, Eggermont J, Droogmans G (2000) Kinetics and pharmacological properties of the calcium-activated chloride-current in macrovascular endothelial cells. Cell Calcium 22:53–63
27. Chartier L, Rankin LL, Allen RE, Kato Y, Fusetani N, Karaki H, Watabe S, Hartshorne DJ (1991) Calyculin-A increases the level of protein phosphorylation and changes the shape of 3T3 fibroblasts. Cell Motil Cytoskeleton 18:26–40
28. Randriamampita C, Tsien RY (1993) Emptying of intracellular Ca^{2+} stores releases a novel small messenger that stimulates Ca^{2+} influx. Nature 364:809–814
29. Shen MR, Chou CY, Hsu KF, Hsu KS, Wu ML (1999) Modulation of volume-sensitive Cl^- channel and cell volume by actin filaments and microtubules in human cervical cancer HT-3 cells. Acta Physiol Scand 167:215–225
30. Essler M, Amano M, Kruse HJ, Kaibuchi K, Weber PC, Aepfelbacher M (1998) Thrombin inactivates myosin light chain phosphatase via Rho and its target Rho kinase in human endothelial cells. J Biol Chem 273:21867–21874
31. Manolopoulos GV, Prenen J, Droogmans G, Nilius B (1997) Thrombin potentiates volume-activated chloride currents in pulmonary artery endothelial cells. Pflugers Arch 433:845–847
32. Nilius B, Prenen J, Walsh MP, Carton I, Bollen M, Droogmans G, Eggermont J (2000) Myosin light chain phosphorylation-dependent modulation of volume-regulated anion channels in macrovascular endothelium. FEBS Lett 466:346–350
33. Akasu T, Ito M, Nakano T, Schneider CR, Simmons MA, Tanaka T, Tokimasa T, Yoshida M (1993) Myosin light chain kinase occurs in bullfrog sympathetic neurons and may modulate voltage-dependent potassium currents. Neuron 11:1133–1145
34. Shen MR, Chou CY, Browning JA, Wilkins RJ, Ellory JC (2001) Human cervical cancer cells use Ca^{2+} signalling, protein tyrosine phosphorylation and MAP kinase in regulatory volume decrease. J Physiol (Lond) 537:347–362